DETERMINATION OF FAILURE MECHANISMS AND DUCTILITY OF 3D STEEL FRAMES UNDER EARTHQUAKE LOADS WITH THREE COMPONENTS

K. Ozakgul

Res. Assist. Dr., Dept. of Civil Engineering , Istanbul Technical University, Istanbul. Turkey
Email: ozakgulk@itu.edu.tr

ABSTRACT :

In this study, it has been aimed to develop an algorithm that determines failure mechanisms and ductility capacities of 3D frames under earthquake loads with three components and a computer program which performs dynamic analysis according to this algorithm. The proposed analysis accounts for material, geometric and connection nonlinearities. Material nonlinearity have been modeled by the Ramberg-Osgood relation. While the geometric nonlinearity caused by axial force has been described by the use of the geometric stiffness matrix, the nonlinearity caused by the interaction between the axial force and bending moment has been also described by the use of the stability functions. The independent hardening model given by Kishi and Chen has been used to describe the nonlinear behaviour of semi-rigid connections.

KEYWORDS: Ramberg-Osgood, independent hardening model, stability functions, ductility demand, yield surface, dissipated energy.

1. INTRODUCTION

Advanced analyses for two dimensional steel frames with semi-rigid connection are carried out by Kishi and Chen (1990) and Barsan and Chiorean (1999). Second-order inelastic analysis for space steel frames with rigid connections are proposed by Orbison et al. (1982), Kim et al. (2001) and Kim et al. (2006). The stability functions are used to capture the second-order effects to minimize modeling and solution time. The nonlinear analysis for the space steel frames with semi-rigid connections is developed by Kim and Choi (2001). These solution methods incorporate geometric and material nonlinearities and the nonlinearity caused by the presence of flexible joints under static loads. A second-order spread-of-plasticity analysis method for three dimensional steel frames is performed by Jiang et al. (2002). Although the plastic zone solution is known as the “exact solution”, it is not be used in daily engineering design because of its highly computational cost.

In this study, the section of members is assumed to be compact which can develop full plastic moment capacity without local buckling. The reduction of torsional stiffness is considered in plastic hinge. Warping torsion is ignored. Lateral torsional buckling of members is assumed to be prevented by adequate lateral braces. Bowing effect is considered.

2. MATERIAL NONLINEARITY

Material nonlinearity is modeled by using the concentrated plastic hinge approach. Plastic hinges are formed when the cross-sectional forces satisfy the plasticity criterion, which is expressed by a force-space interaction function. For steel beam-columns with compact I-shaped sections, the plastic interaction functions proposed by Morris and Fenves (1969) are used as shown in Fig. 1. Yield surface expressions for the I-shaped cross-section are formulated with respect to a various position of the neutral axis (Morris and Fenves 1969). These expressions were preferred instead of approximate equations for wide-flange I sections, because the expressions below are valid not only for wide-flange but also for all types of I sections.

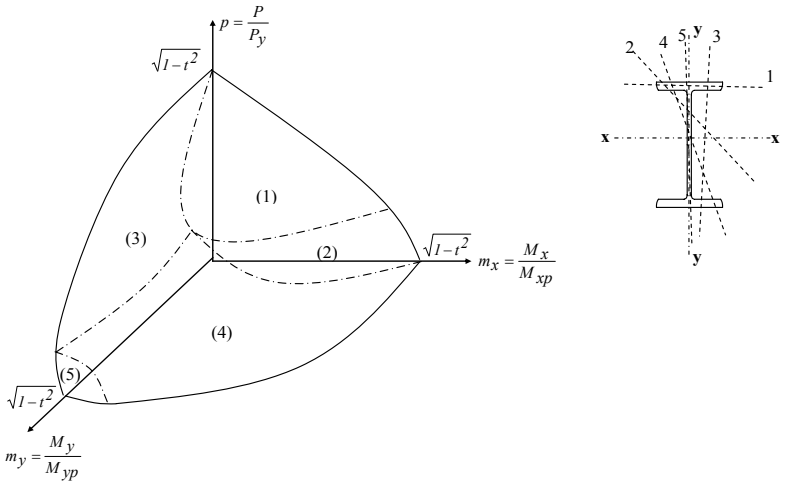

Figure 1 Full plastification surface

$p = P / P_y$, the ratio of the axial force to the squash load; $m_x = M_x / M_{xp}$, the ratio of the strong axis bending moment to the corresponding plastic moment; $m_y = M_y / M_{yp}$, the ratio of the weak axis bending moment to the corresponding plastic moment; $t = T / T_p$, the ratio of the torsional moment to the plastic torsional moment.

2.1. Elasto-Plastic Tangent Stiffness Matrix

The stress-strain relations for nolinear material behaviour is modelled by following equation which corresponds essentially to the inverse of the Ramberg-Osgood representation.

$$\sigma = \frac{E \cdot \varepsilon}{\left[1 + \left|\frac{E \cdot \varepsilon}{\sigma_u}\right|^n\right]^{1/n}} \tag{2.1}$$

where σ and ε are normal stress and strain, E is Young's modulus, σ_u is the ultimate stress and n is constant defining shape of stress-strain relationship. The response in torsion and shear is assumed linearly elastic. The moment-effective rotation relationship proposed by Goldberg and Richard (1963) for each bending directions x and y and axial force-axial deformation relationship is expressed in the same form as the stress-strain equation.

The incremental force-displacement equation may be written for the three-dimensional elasto-plastic beam-column element as,

$$\begin{Bmatrix} \Delta P \\ \Delta T \\ \Delta M_{xi} \\ \Delta M_{xj} \\ \Delta M_{yi} \\ \Delta M_{yj} \end{Bmatrix} = \begin{bmatrix} \frac{EA}{L}\Big/g & 0 & 0 & 0 & 0 & 0 \\ 0 & \frac{GJ}{L} & 0 & 0 & 0 & 0 \\ 0 & 0 & \frac{4EI_x}{L}\Big/p & \frac{2EI_x}{L}\Big/r_1 & 0 & 0 \\ 0 & 0 & \frac{2EI_x}{L}\Big/r_1 & \frac{4EI_x}{L}\Big/s & 0 & 0 \\ 0 & 0 & 0 & 0 & \frac{4EI_y}{L}\Big/h & \frac{2EI_y}{L}\Big/r_2 \\ 0 & 0 & 0 & 0 & \frac{2EI_y}{L}\Big/r_2 & \frac{4EI_y}{L}\Big/d \end{bmatrix} \cdot \begin{Bmatrix} \Delta(\Delta L) \\ \Delta\theta_T \\ \Delta\phi_{xi} \\ \Delta\phi_{xj} \\ \Delta\phi_{yi} \\ \Delta\phi_{yj} \end{Bmatrix} \tag{2.2}$$

where M and ϕ are bending moment and the corresponding rotation; P and ΔL are axial force and axial deformation; T and θ_T are torsional moment and torsional rotation; A, I_x, I_y and L are area, moment of inertia with

respect to x and y axis, and length of beam-column element; E, G and J are elastic modulus, shear modulus and torsional constant of material; g, d, h, p and s appearing in the tangent stiffness matrix are the elasto-plastic correction factors (Uzgider 1980); $r_1 = 2ps/(p+s)$, $r_2 = 2hd/(h+d)$. These variables are defined to modify the member stiffness at the each time increment.

3. GEOMETRIC NONLINEARITY

While the geometric nonlinearity of frame *(P-Δ)* caused by axial force has been described by the use of the geometric stiffness matrix, the nonlinearity of member *(P-δ)* caused by the interaction between the axial force and bending moment has been also described by the use of the stability functions (Kim et al. 2001).

The element geometric stiffness matrix is composed of the changes in nodal forces due to second order effects *(P-Δ)* of axial nodal forces in case of rigid body rotation of the frame element.

Stability functions are used to capture the second-order effects since they can account for the stiffness degradation caused by the interaction effect between the axial force and bending moments. S_1 is stability function for the effect of flexure on axial stiffness (bowing effect). S_2, S_3, S_4 and S_5 are stability functions for the effect of axial force on flexural stiffness with respect to x and y axes, respectively (Ekhande et al. 1989). The force-displacement equation using stability functions may be written for the three-dimensional elasto-plastic beam-column element as

$$\begin{Bmatrix} \Delta P \\ \Delta T \\ \Delta M_{xi} \\ \Delta M_{xj} \\ \Delta M_{yi} \\ \Delta M_{yj} \end{Bmatrix} = \begin{bmatrix} S_1\frac{EA}{L}\Big/g & 0 & 0 & 0 & 0 & 0 \\ 0 & \frac{GJ}{L} & 0 & 0 & 0 & 0 \\ 0 & 0 & S_2\frac{4EI_x}{L}\Big/p & S_3\frac{2EI_x}{L}\Big/r_1 & 0 & 0 \\ 0 & 0 & S_3\frac{2EI_x}{L}\Big/r_1 & S_2\frac{4EI_x}{L}\Big/s & 0 & 0 \\ 0 & 0 & 0 & 0 & S_4\frac{4EI_y}{L}\Big/h & S_5\frac{2EI_y}{L}\Big/r_2 \\ 0 & 0 & 0 & 0 & S_5\frac{2EI_y}{L}\Big/r_2 & S_4\frac{4EI_y}{L}\Big/d \end{bmatrix} \cdot \begin{Bmatrix} \Delta(\Delta L) \\ \Delta\theta_T \\ \Delta\phi_{xi} \\ \Delta\phi_{xj} \\ \Delta\phi_{yi} \\ \Delta\phi_{yj} \end{Bmatrix} \quad (3.1)$$

4. SEMI-RIGID CONNECTION MODELING

In this study, the independent hardening model is used to simulate the nonlinear connection behaviour under dynamic loading, as presented by Sekulovic et al. (2002). The moment-rotation curve under the first cycle of loading, unloading and reverse loading remain unchanged under the repetition of loading cycles. The skeleton curve used in the model is obtained from the three-parameter power model proposed by Kishi and Chen (1990).

The three parameter power model contains three parameters: initial connection stiffness R_{ki}, ultimate connection moment capacity M_u and shape parameter n. To determine the three parameters for given connection type, practical procedures proposed by Kishi and Chen (1990) are used. Type of semi-rigid connection that is considered herein is the top and seat angle with double web-angle connection (TSDWA).

A beam-column element with semi-rigid connections is shown in Fig. 2. The flexible connections are represented by rotational springs at beam ends. The connection spring element is assumed massless and dimensionless in size. R_{xi}, R_{yi}, R_{xj} and R_{yj} are tangent stiffness of the connections at the i and j ends of the beam-column element in the x-x and y-y direction, respectively. Values of R_{xi}, R_{yi}, R_{xj} and R_{yj} are to be obtained from the independent hardening model.

The element tangent stiffness matrix represented by Eqn. 3.1 is modified to account for the effect of the semi-rigid connections in a beam-column element.

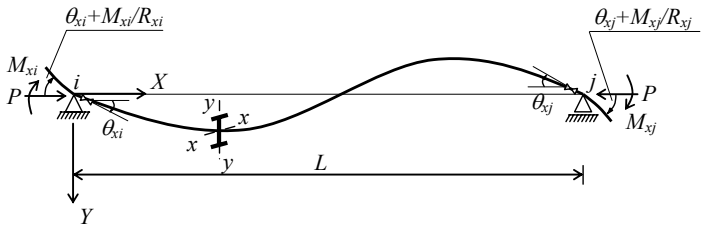

Figure 2 Beam-column element with semi-rigid connection

5. NUMERICAL PROCEDURES

The incremental form of the equation of motion for frames subjected to dynamic is given by

$$\boldsymbol{M}\cdot\Delta\ddot{\boldsymbol{x}}+\boldsymbol{C}\cdot\Delta\dot{\boldsymbol{x}}+\boldsymbol{K}\cdot\Delta\boldsymbol{x}=\Delta\boldsymbol{P} \tag{5.1}$$

In which $\boldsymbol{K}$ is the tangent stiffness matrix for the system of structural elements; $\boldsymbol{M}$ is the mass matrix; $\boldsymbol{C}=\alpha\boldsymbol{M}+\beta\boldsymbol{K}$ is the viscous damping matrix, where α and β are mass and stiffness proportional damping factors, respectively; $\Delta\ddot{\boldsymbol{x}}$, $\Delta\dot{\boldsymbol{x}}$, $\Delta\boldsymbol{x}$ and $\Delta\boldsymbol{P}$ are incremental acceleration, velocity, displacement and externally applied force vectors, respectively, over a time increment of Δt.

The equations of motions are integrated using step-by-step integration, with a constant acceleration assumption within any step (Kim et al. 2006). The dynamic equilibrium of the system in terms of the unknown incremental nodal displacement $\Delta\boldsymbol{x}$ can be expressed as

$$\left[\boldsymbol{K}+\frac{1}{\delta_2\Delta t^2}\boldsymbol{M}+\frac{\delta_1}{\delta_2\Delta t}\boldsymbol{C}\right]\Delta\boldsymbol{x}=\Delta\boldsymbol{P}+\left[\frac{1}{\delta_2\Delta t}\boldsymbol{M}+\frac{\delta_1}{\delta_2}\boldsymbol{C}\right]\dot{\boldsymbol{x}}_t+\left[\frac{1}{2\delta_2}\boldsymbol{M}+\Delta t\left(\frac{\delta_1}{2\delta_2}-1\right)\boldsymbol{C}\right]\ddot{\boldsymbol{x}}_t \tag{5.2}$$

where δ_1 and δ_2 are parameters that can be determined to obtain integration accuracy and stability; $\dot{\boldsymbol{x}}_t$ and $\ddot{\boldsymbol{x}}_t$ are total velocity and acceleration vectors at time t. The constant-average-acceleration method, in which $\delta_1 = ½$ and $\delta_2 = ¼$, has the most desirable accuracy characteristics.

When the incremental displacement $\Delta\boldsymbol{x}$ at time $t+\Delta t$ in the Eqn. 5.2 is solved, it is used to update the acceleration, the velocity, the displacement and the force vectors. This procedure is repeated for the next time increments until the considered frame system collapses or the desired duration in the time history is reached.

6. ENERGY RESPONSE EVALUATION

The input energy in the system due to seismic loading, dissipated energy by the hysteretic behaviour of the material at the location of plastic hinges, if they form, by viscous damping and by hysteretic behaviour of the semi-rigid connections, elastic strain energy and kinetic energy have been described as

$$E_I(t)=E_E(t)+E_D(t)+E_{Dis}(t)+E_K(t) \tag{6.1}$$

where $E_I(t)$ is seismic input energy, $E_E(t)$ is elastic strain energy, $E_D(t)$ is damping energy, $E_{Dis}(t)$ is dissipiate energy and $E_K(t)$ is kinetic energy. As presented by Sekulovic and Nefovska-Danilovic (2008), these energy terms are expressed as follows:

$$E_I(t)=-\int_0^x \boldsymbol{M}\ \boldsymbol{II}\ \ddot{x}_g\,d\boldsymbol{x}=-\int_0^t \dot{\boldsymbol{x}}^{\mathrm{T}}\boldsymbol{M}\ \boldsymbol{II}\ \ddot{x}_g\,dt \tag{6.2}$$

$$E_E(t) = \frac{1}{2}\,\dot{\boldsymbol{x}}_e{}^T \boldsymbol{K}_e \boldsymbol{x}_e \tag{6.3}$$

$$E_D(t) = \int_0^x \boldsymbol{C}\ \dot{\boldsymbol{x}}\ d\boldsymbol{x} = \int_0^t \dot{\boldsymbol{x}}^{\mathrm{T}} \boldsymbol{C}\ \dot{\boldsymbol{x}}\ dt \tag{6.4}$$

$$E_{Dis}(t) = \int_0^x \boldsymbol{K}\ \boldsymbol{x}\ d\boldsymbol{x} - E_E(t) = \int_0^t \dot{\boldsymbol{x}}^{\mathrm{T}} \boldsymbol{K}\ \boldsymbol{x}\ dt - E_E(t) \tag{6.5}$$

$$E_K(t) = \frac{1}{2}\,\dot{\boldsymbol{x}}^T \boldsymbol{M}\,\dot{\boldsymbol{x}} \tag{6.6}$$

where $\boldsymbol{K}_e$ and $\boldsymbol{x}_e$ are the elastic stiffness matrix and elastic displacement vector, $\boldsymbol{dx}$ is incremental displacement vector, $\boldsymbol{x}$ and $\dot{\boldsymbol{x}}$ are total displacement and velocity vectors at time t, $\boldsymbol{II}$ is the matrix that matches the earthquake acceleration components to the corresponding nodal degrees of freedom.

7. ESTIMATION OF DUCTILITY DEMANDS

The estimation of the ductility demands under seismic loading conditions and the prediction of ductility capacity have become an important subject in the design of structures. The ductility demands may be determined from the inelastic analysis of the structures (Lee et al. 1997).

Rotational ductility is defined by the ratio of the maximum rotation θ_{max} at the end of a member to the yield rotation θ_y as follows,

$$\mu_\theta = \frac{\theta_{max}}{\theta_y} \tag{7.1}$$

The system level ductility is defined by the ratio of the maximum system displacement u_{max} to the yield displacement u_y as,

$$\mu_{sys} = \frac{u_{max}}{u_y} \tag{7.2}$$

8. NUMERICAL EXAMPLE

For the numerical example, three-dimensional steel frames presented by Kim et al. (2006) are used. The earthquake records with three components of the San Fernando 1971 (station: Pacoima Dam) are used as ground motion input data in the present study. The mass and stiffness proportional damping factors are chosen corresponding to 5% viscous damping ratio. In numerical modeling, each member of the space frames is only modeled by one element. The results of the linear analysis of the numerical examples with rigid joints obtained by this study have been compared with the corresponding results obtained by the commercial finite element analysis software SAP2000. It can be seen that the two sets of results are very close.

8.1. Two-story One-bay Space Frame

The geometric properties and other pertinent information of this frame with lumped masses at the nodes are given in Fig. 3. The static gravitational loads are applied at all frame nodes to demonstrate the second-order effects in a clear manner. All sections are H125x125x6.5x9.

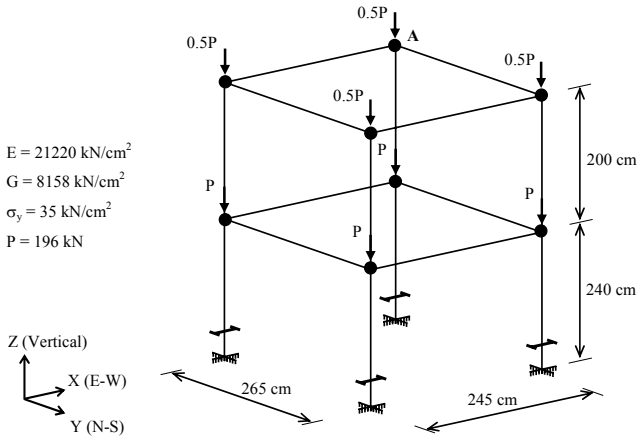

Figure 3 Two-story one-bay space frame

The displacement responses along *x*-axis of node A of the frame with semi-rigid connection and rigid jointed frame according linear and second-order elastoplastic analyses are shown in Fig. 4.

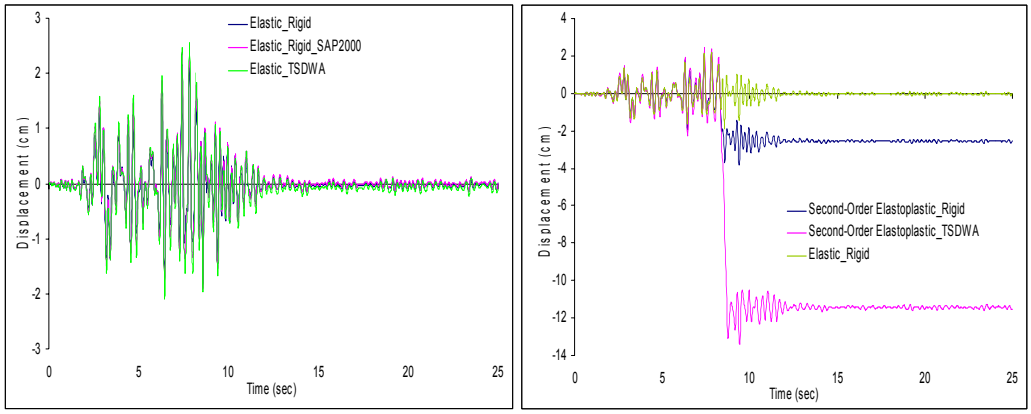

a **b**

Figure 4 Displacement response (x_A) of two story frame according to the (a) elastic analyses and (b) inelastic analyses

The inelastic behaviour of the framed structure for the second-order elastoplastic analysis case under San Fernando earthquake can be seen that the column end moments in the frame almost reach the column moment capacity, therefore plastic hinges form. The locations of plastic hinges are shown in Fig. 5.

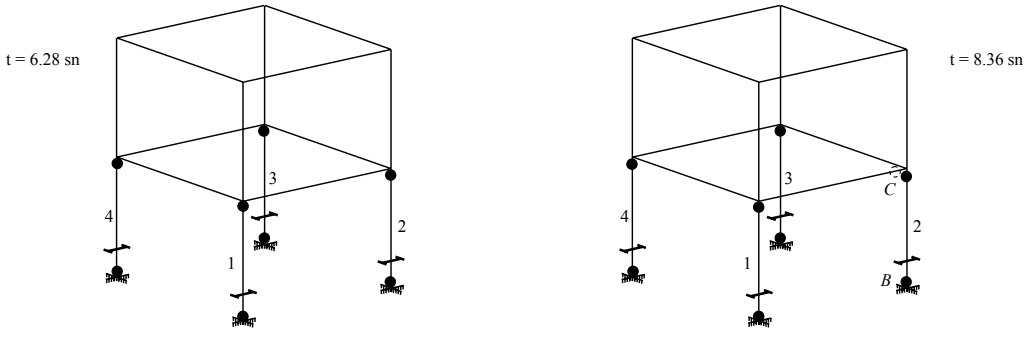

a **b**

Figure 5 The locations of plastic hinges of two story frame subjected to San Fernando earthquake (a) rigid connections, (b) semi-rigid connections

The hysteretic moment-rotation loops at node B where the member begins to yield and the hysteretic connection loop at node C are shown in Fig. 6, respectively.

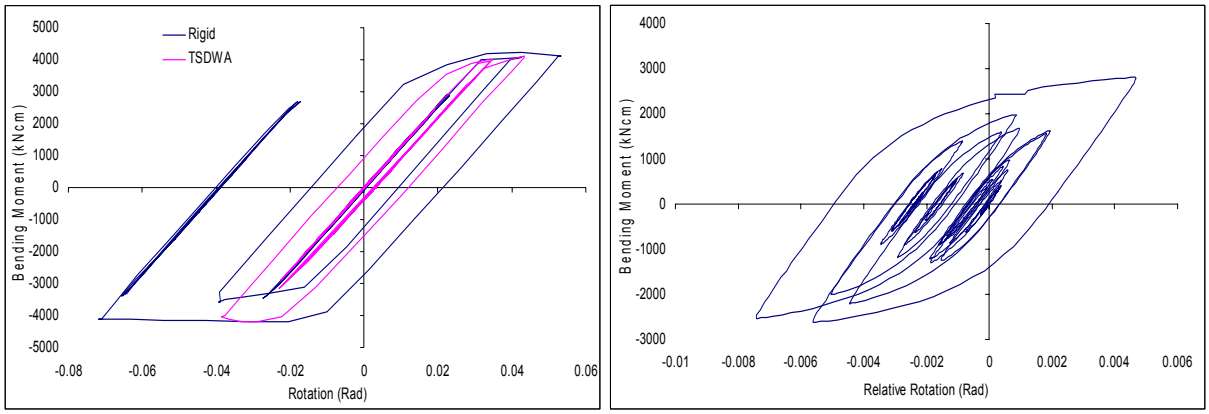

a **b**

Figure 6 The hysteretic loops (a) at point B and (b) at point C

The based shear force-roof displacement relationships along *X*-axis and *Y*-axis of the rigid jointed frame obtained by proposed computer program are shown in Fig. 7, respectively. The system-level ductility demands estimated by the force-displacement relationships are shown in Table 8.1 along with maximum local ductility demands.

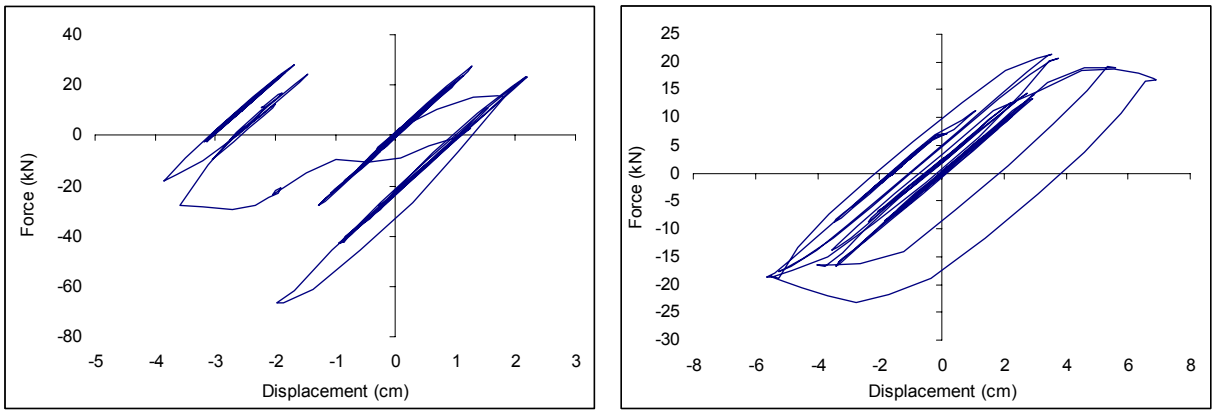

a **b**

Figure 7 Force-displacement relationships (a) along *X*-axis and (b) along *Y*-axis

Table 8.1 Rotational ductility demands and system ductility demands

Ductility demands of frame with rigid connections						Ductility demands of frame with semi-rigid connections					
Rotational Ductility				System Ductility		Rotational Ductility				System Ductility	
Member Id.				Along *X*-axis	Along *Y*-axis	Member Id.				Along *X*-axis	Along *Y*-axis
1	2	3	4			1	2	3	4		
13.6	13.9	13.7	13.7	3.36	1.53	5.14	3.75	3.74	5.22	2.51	1.46

Results of the energy response of the frame with rigid and semi-rigid connections is shown in Fig. 8. Viscous damping energy constitutes 65% of input energy, while dissipated energy constitutes 30% of input energy for the frame with semi-rigid joints. For the frame with rigid joints, while viscous damping energy rises up to 74% of input energy, the ratio for dissipated energy decreases to 20%.

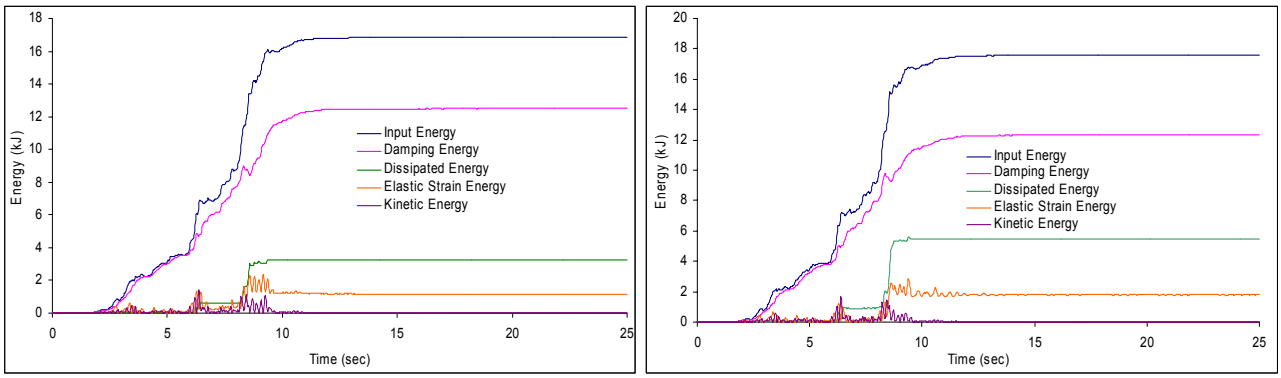

Figure 8 Energy response of two story frame with (a) rigid connections and (b) semi-rigid connections

9. CONCLUSION

In this study, an effective algorithm for second-order elastoplastic dynamic time-history analysis of three dimensional steel frames has been presented. The system-level ductility demands of the multistory steel structures are found to be about 1/4~1/2 of those for the element-level. The results of energy responses show that semi-rigid connections increase the overall structural energy dissipation capacity, which is very important for a structure to overcome under earthquake induced seismic loads.

REFERENCES

Barsan, G.M. and Chiorean, C.G. (1999). Computer program for large deflection elasto-plastic analysis of semi-rigid steel frameworks. *Computers & Structures* **72**, 699-711.
Ekhande, S.G., Selvappalam, M. and Madugula, M.K.S. (1989). Stability Functions for Three-Dimensional Beam-Columns. *ASCE Journal of Structural Division* **115**, 467-479.
Goldberg, J.E. and Richard, R.M. (1963). Analysis of Nonlinear Structures. *ASCE Journal of the Structural Division* **89**, 333-351.
Jiang, X.M., Chen, H. and Liew, J.Y.R. (2002). Spread-of-plasticity analysis of three dimensional steel frames. *Journal of Constructional Steel Research* **58:2**, 193-212.
Kim, S.E. and Choi, S.H. (2001). Practical advanced analysis for semi-rigid space frames. *International Journal of Solids and Structures* **38**, 9111-9131.
Kim, S.E., Ngo-Huu, C. and Lee, D.H. (2006). Second-order inelastic dynamic analysis of 3-D steel frames. *International Journal of Solids and Structures* **43**, 1693-1709.
Kim, S.E., Park, M.H. and Choi, S.H. (2001). Direct design of three-dimensional frames using practical advanced analysis. *Engineering Structures* **23**, 1491-1502.
Kishi, N. and Chen, W.F. (1990). Moment-rotation relations of semi-rigid connections with angles. *ASCE Journal of Structural Engineering* **116**, 1813-1834.
Lee, D.G., Song, J.K. and Yun, C.B. (1997). Estimation of System-Level Ductility Demands for Multi-Story Structures. *Engineering Structures* **19**, 1025-1035.
Morris, G.A. and Fenves, S.J. (1969). Approximate yield surface equations. *ASCE Journal of the Engineering Mechanics Division* **95**, 937-954.
Orbison, J.G., McGuire, W. and Abel, J.F. (1982). Yield surface applications in nonlinear steel frame analysis. *Computer Methods in Applied Mechanics and Engineering* **33**, 557-573.
Sekulovic, M. and Nefovska-Danilovic, M. (2008). Contribution to transient analysis of inelastic steel frames with semi-rigid connections. *Engineering Structures* **30**, 976-989.
Sekulovic, M., Salatic, R. and Nefovska, M. (2002). Dynamic analysis of steel frames with flexible connections. *Computers & Structures* **80**, 935-955.
Uzgider, E.A. (1980). Inelastic response of space frames to dynamic loads. *Computers & Structures* **11,** 97-112.